The nature of fluorescence emission in the red fluorescent protein DsRed, revealed by single-molecule detection

M. F. Garcia-Parajo*†, M. Koopman*, E. M. H. P. van Dijk*, V. Subramaniam‡, and N. F. van Hulst*

*Applied Optics Group, Department of Applied Physics and MESA+ Research Institute, University of Twente, P.O. Box 217, 7500 AE Enschede, The Netherlands; and ‡Department of Molecular Biology, Max Planck Institute for Biophysical Chemistry, 37070 Göttingen, Germany

Communicated by Michael Kasha, Florida State University, Tallahassee, FL, October 3, 2001 (received for review June 22, 2001)

Recent studies on the newly cloned red fluorescence protein DsRed from the *Discosoma* genus have shown its tremendous advantages: bright red fluorescence and high resistance against photobleaching. However, it has also become clear that the protein forms closely packed tetramers, and there is indication for incomplete protein maturation with unknown proportion of immature green species. We have applied single-molecule methodology to elucidate the nature of the fluorescence emission in the DsRed. Real-time fluorescence trajectories have been acquired with polarization sensitive detection. Our results indicate that energy transfer between identical monomers occurs efficiently with red emission arising equally likely from any of the chromophoric units. Photodissociation of one of the chromophores weakly quenches the emission of adjacent ones. Dual color excitation (at 488 and 568 nm) single-molecule microscopy has been performed to reveal the number and distribution of red vs. green species within each tetramer. We find that 86% of the DsRed contain at least one green species with a red-to-green ratio of 1.2–1.5. On the basis of our findings, oligomer suppression would not only be advantageous for protein fusion but will also increase the fluorescence emission of individual monomers.

The cloning of the red fluorescent protein (drFP583, commercially available as DsRed) from the Indo pacific reef coral *Discosoma* sp (1) has triggered intense biological interest as a potential expression marker and fusion partner that would be complementary to the *Aequorea victoria* green fluorescent protein (*av*GFP). The main advantage of these naturally fluorescent proteins is that they provide strong visible fluorescence and can be genetically fused to other proteins. Since the cloning of the *av*GFP (2, 3), different mutants have been produced to extend the palette of available colors. However, no GFP mutant has been produced with emission maxima longer than 529 nm (3). The newly cloned DsRed has bright red fluorescence with emission maxima at 583 nm, one of the longest wavelength emissions reported so far in a wild-type species [Fradkov *et al.* (4) have reported a wild type highly homologous to the drFP583 with 593-nm emission and a hybrid with 616-nm emission]. Potentially, DsRed is an ideal partner of GFP in fluorescence resonance energy transfer (FRET) experiments, particularly in cell biological applications in which cellular autofluorescence poses a problem (5).

In the last few months, extensive research has been done in the biochemical and photophysical investigation of DsRed. The absorption spectrum of the mature protein exhibits a strong band with a peak at 558 nm and two minor shoulders at 526 and 490 nm (6). An extinction coefficient of 75,000 mol^{-1}/cm^{-1} and a fluorescence quantum yield of 0.7 at 558-nm excitation wavelength have been reported (7), much higher than initially published by Matz *et al.* (1). The protein proves to be stable under harsh pH conditions and is extremely resistant to photobleaching (7, 8). However, two major deficiencies have been discovered: the slow and possibly incomplete maturation for the red fluorescence, which apparently passes through an obligatory green-emitting intermediate similar to *av*GFP, and its tendency to oligomerize even at dilute concentrations (7, 9, 10). Yeast two-hybrid assays and cell expression also indicate oligomerization and/or aggregation in living cells (7, 9).

Recently, the crystal structure of DsRed became available and supports the tetramerization of the protein (11, 12). The four chromophores in the tetramer form an antenna-like rectangular array of $\approx 2.7 \times 3.4$ nm, hinting at the possibility of strong coupling between the chromophores. From the crystal structure, Wall *et al.* (11) estimated angles of 21°, 47°, and 41° between different pairs of the tetramer, strengthening the hypothesis of energy transfer between different subunits. Time-resolved fluorescence anisotropy experiments at 490-nm excitation wavelength showed a biexponential decay with a fast decay of 211 ps and a slow rotational time of 53 ns (6). The slow rotational time was attributed to the tetrameric structure. The fast depolarization component has two possible origins: intratetramer energy transfer between nonparallel transition dipoles or internal rotation of the chromophores within the polypeptide shell or relative to the adjacent chromophores, as in the red-shifted GFP mutant (13). The workers favored the first hypothesis (6). Picosecond time-resolved experiments in solution (50% glycerol) confirmed FRET between green and red species within the tetramer (14).

Even when FRET between green and red species of DsRed has been observed, it is not known how the emission between fully red monomers occurs and how many red species within the tetramer contribute to the fluorescence. Mass spectrometry indicated that after prolonged incubation, the tetramer might contain green and red species in a 1:1 ratio, which the workers interpreted as incomplete maturation of DsRed (10, 12). The reasons for this "incomplete maturation" are not known. It is also not known whether individual tetramers consist of a random or a deterministic composition of green vs. red monomers. The biological significance of all these questions is 2-fold. On the one hand, it is of immediate relevance to any FRET experiment to quantify the degree of crosstalk caused by intratetrameric FRET. On the other hand, if mutagenesis succeeds in producing monomers of DsRed, it will be important to determine the proportion of green vs. red fluorescent species and their respective photophysical properties.

We have used single-molecule methodology to elucidate the nature of the fluorescence emission in DsRed. This technique is extremely powerful in revealing photodynamic properties in molecular systems by avoiding population averaging (15). Features hidden in the ensemble, such as rare fluctuations and on–off blinking, have been directly observed, including the case of GFP (16, 17). Our single-molecule DsRed data show the multistep emission characteristic of closely packed multichromophoric systems, consistent with recent DsRed experiments (8,

Abbreviations: GFP, green fluorescent protein; FRET, fluorescence resonance energy transfer.

†To whom reprint requests should be addressed. E-mail: m.f.garciaparajo@tn.utwente.nl.

The publication costs of this article were defrayed in part by page charge payment. This article must therefore be hereby marked "*advertisement*" in accordance with 18 U.S.C. §1734 solely to indicate this fact.

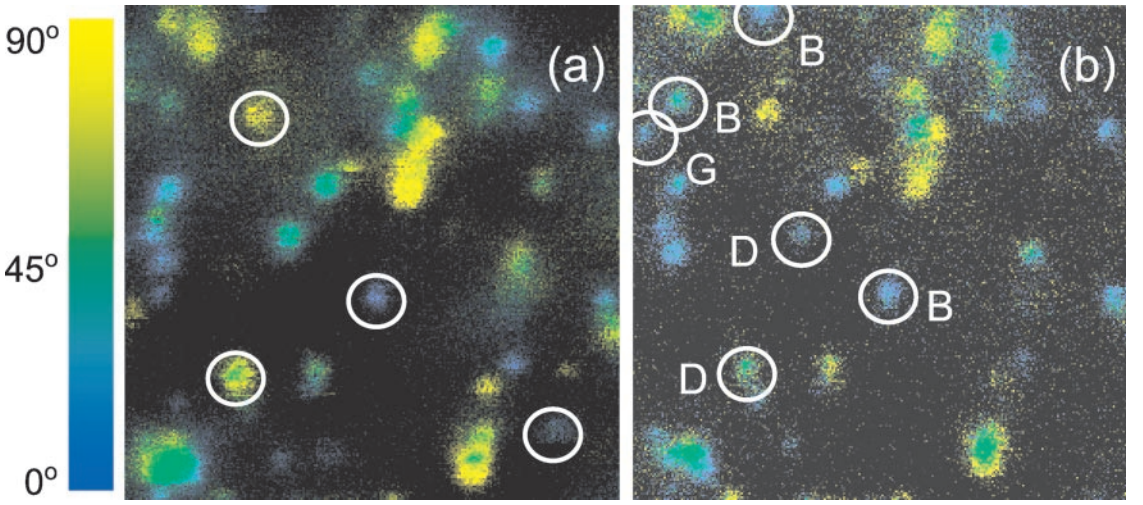

Fig. 1. Near-field fluorescence images of individual DsRed molecules embedded in a poly(acrylamide) gel. Both images correspond to the same area in the sample, 3.2 × 3.2 μm^2, 256 × 256 pixels, and $\lambda_{det} > 590$ nm. (*a*) Circularly polarized excitation at 568 nm, 0.7 kW/cm^2, and integration time of 5 ms/pixel. Circles highlight molecules that exhibit intermittent emission and photodissociation. (*b*) Circularly polarized excitation at 488 nm, 0.3 kW/cm^2, and 10 ms/pixel. Molecules labeled B are comparatively brighter in *b* than in *a*, whereas molecules labeled D are comparatively dimmer.

18). From our polarization-dependent single-molecule fluorescence trajectories, we find information about the type of interactions between different chromophores constituting the complex. We base the analysis on the assumption that, under our experimental conditions, DsRed remains a tetramer. With this assumption, our data fit nicely to a model in which energy transfer between red monomers of the tetramer governs fluorescence emission. We also provide answers to the number and distribution of green vs. red species within each tetramer. In its final state, DsRed seems to be composed of two different chromophores with a 1.2–1.5 red-to-green ratio.

Materials and Methods

The DNA sequence encoding for DsRed was excised from the pDsRed1-N1 plasmid (CLONTECH) and inserted into the pRSETa (Invitrogen) vector. These plasmids code for expression of fluorescent proteins with an additional six histidines at the amino terminus, under the control of the T7 promoter inducible by isopropyl-β-D-thiogalactoside (IPTG). *Escherichia coli* BL21 (DE3) cells were transformed with the plasmids according to standard protocols and grown in LB medium at 37°C by using ampicillin for selection. Protein expression was induced by 1 mM IPTG. Cells were typically grown further for 12–24 h after induction to allow the DsRed protein to mature completely. The recombinant proteins with a 6-histidine tag were purified on a Ni-chelating resin (Ni-NTA-Agarose, Qiagen, Hilden, Germany) by using standard procedures. The purified protein was dialyzed against 100 mM Tris·HCl buffer, pH 8.5, containing 100 mM NaCl. Protein purity was checked by gel electrophoresis and gel filtration and indicated a homogeneous preparation. Samples for single-molecule experiments were prepared by immobilizing the proteins [10^{-8} M in water-filled pores of poly(acrylamide)], following a procedure similar to that described in ref. 17.

Single-molecule experiments were performed by using a near-field scanning optical microscope (NSOM). In this technique, an aperture probe of dimensions smaller that the excitation wavelength is used to illuminate the sample (19). Light from a Ar^+–Kr^+ ion laser was coupled to the back side of the NSOM probe (single-mode fiber, λ = 630 nm, Cutz, Frankfurt, Germany). The fluorescence emission of the individual proteins was collected by a Zeiss 1.3 N.A./×63 oil-immersion objective and, after selection by suitable fluorescence filters ($\lambda_{det} > 590$ nm), it was separated in two perpendicular polarization components and focused onto two avalanche photodiodes (SPCM-100, EG & G, Quebec, Canada). Details about the experimental setup can be found elsewhere (19). Integration time for imaging was 5 ms/pixel. Fluorescence time trajectories were obtained by positioning the molecules in the center of the excitation profile and continuously recording the fluorescence emission in the two polarization channels with 1-ms dwell times for 100 s.

Single-molecule two-color excitation experiments with polarization sensitive detection were carried out by illuminating the same sample area with circularly polarized light sequentially with 568 nm, 488 nm, and back to 568 nm. Only fluorescence emission above 590 nm was detected, because emission in the green band on excitation at 488 nm is negligible (4–5% of the red peak intensity, as estimated from the ensemble emission spectra). Fluorescence images were generated by using a pseudo-color coding, blue for the 0° avalanche photodiode detector (*x*-direction) and yellow for the 90° detector (*y*-direction). The color of each fluorescent spot reflects the relative contribution of each polarization component and thus the in-plane orientation of the chromophore emission dipole, whereas the brightness is a measure of the total fluorescence intensity. For analysis of the polarization measurements, we have defined the degree of polarization P as $(I_x - GI_y)/(I_x + GI_y)$, where I_x and I_y are the emission components detected in the parallel and perpendicular polarized directions, respectively, and G is a correction factor that accounts for the difference in sensitivity of both detectors. In general, P reflects the in-plane orientation of the emission dipole moment of a molecule. Values of P vary from -1 for a molecule oriented along the 90° channel (*y*-direction) to $+1$ for a molecule oriented along the 0° channel (*x*-direction).

Bulk photobleaching experiments were performed by using 70 μl of DsRed in a 3-mm path-length cuvette and overlaid with paraffin oil to prevent evaporation. The protein was illuminated with ≈50 mW of the 568-nm line from the Ar^+–Kr^+ ion laser for various periods of time (1 and ≈3 h). Absorption, fluorescence emission, and excitation spectra were taken before and after photobleaching (fluorescence emission with λ_{exc} = 480 nm and fluorescence excitation with λ_{det} = 650 nm).

Results and Analysis

Single-Molecule Microscopy. Fig. 1*a* shows a near-field fluorescence image of spatially distributed individual DsRed molecules embedded in the gel and excited with 568 nm. The image exhibits the

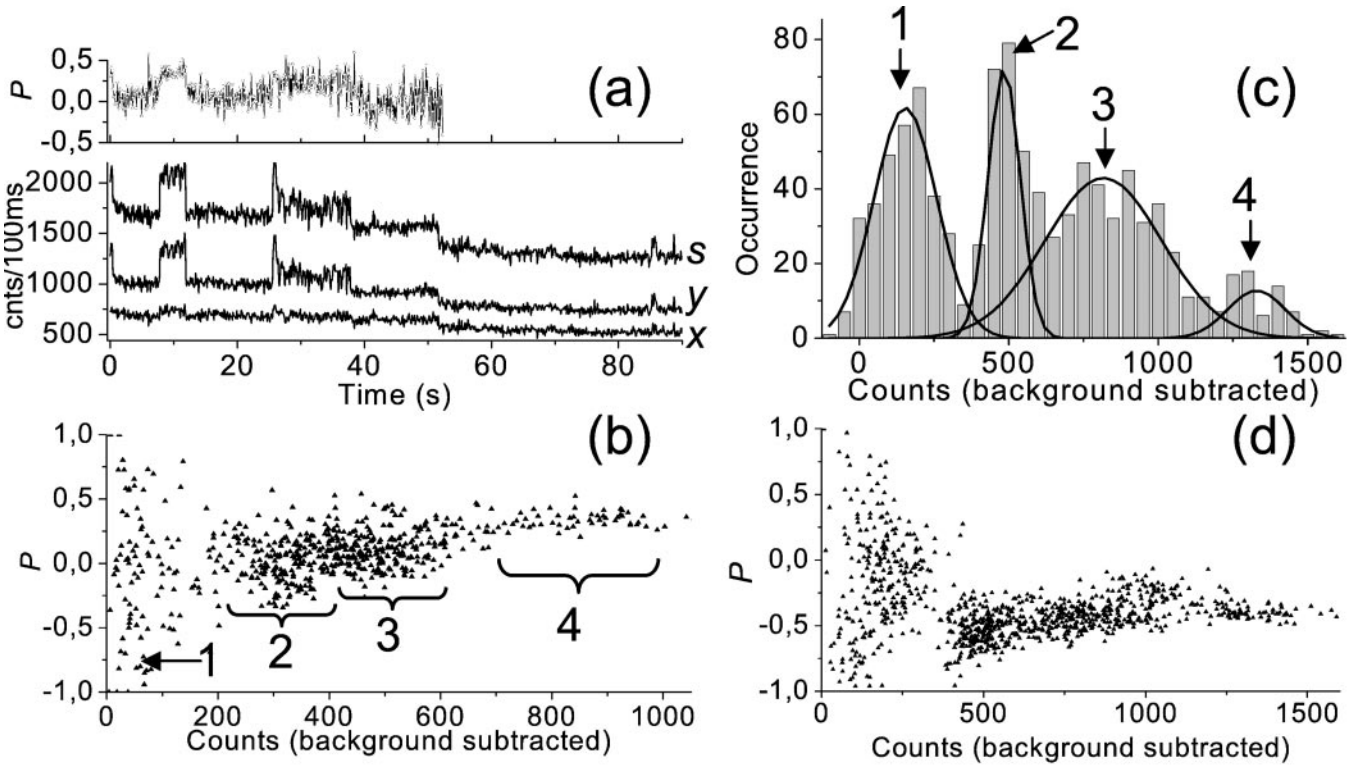

Fig. 2. (*a*) Real-time fluorescence trajectory in both polarization channels of a DsRed molecule. Excitation intensity was 0.5 kW/cm^2. Acquisition time was 1 ms per point, although the signal has been binned to 100 ms per point to reduce noise. The total emitted signal *s* is obtained by adding the counts of both *x* and *y* detectors. The real-time degree of polarization *P* is shown in upper section. (*b*) Correlation plot between *P* and the total number of counts emitted by the molecule in *a*. The clusters of points corresponding to the emission of the four different levels are marked on the plot. (*c*) Histogram of the total number of counts of another DsRed molecule exhibiting four intensity levels. The peak values of the intensity (after fitting to gaussians) are: 1,329 (w = 192), 816 (w = 392), 484 (w = 107), and 153 (w = 210), for the fourth, third, second, and first levels, respectively, where w is the width of the Gaussian. (*d*) *P* vs. total number of counts for molecule in *c*.

features characteristic of single-molecule emission, i.e., intermittent on–off emission and discrete cessation (photobleaching) of the fluorescence of some molecules and unique dipole emission of all molecules, evidenced by the constant color of each individual spot. A constant color per spot also indicates that the proteins are immobilized in the gel, and rotational diffusion does not occur on the time scale of our experiments. The existence of spots with different colors (blue to yellow) and discrete fluorescence behavior are actually surprising if one considers that the fluorescence arises not from one single molecule but from the emission of four chromophores, each with a defined dipole emission. The simplest explanation for our results is to consider that, at the low concentrations used in our experiments (10^{-8} M), DsRed exists as monomers instead of tetramers. In principle, possibilities that include three of four chromophores being in a green and/or nonfluorescent state should also be taken into account. At first glance, however, their occurrence is somewhat improbable, considering the weak absorption band at 488 nm and the bright red fluorescence in solution observed with the samples used in our single-molecule experiments.

To assess the relative contribution of green species to the total red emission, we excited the same population of individual proteins with both 488 nm (excitation of green and red species via FRET) and 568 nm (excitation of red species only) excitation. In both cases, the fluorescence was detected at >590 nm by using the same filter set. Fig. 1*b* shows the same area as imaged in Fig. 1*a* but with excitation at 488 nm. Although in general the fluorescence emission with blue excitation is much weaker that with yellow excitation, careful inspection of Fig. 1*b* reveals that some fluorescence spots were comparatively brighter when excited at 488 than at 568 nm and others much weaker. For a total of 96 molecules investigated with both excitation wavelengths, we found that 12.5% of the molecules emitted red fluorescence only when excited at 568 nm, whereas a small number (≈4%) of the molecules emitted red fluorescence only when excited at 488 nm (labeled as G in Fig. 1*b*). The remaining 83.5% of the molecules displayed fluorescence at both excitation wavelengths, although from the images it was hard to extract quantitative information about the fractional increase (or decrease) of red fluorescence on excitation in the blue.

Real-Time Fluorescence Trajectories. Fig. 2*a* shows the fluorescence time trajectory together with the real-time in-plane orientation (degree of polarization *P*) of a DsRed molecule immobilized in the water-pore gel. We used circularly polarized light at 568 nm to equally excite all possible in-plane-oriented red monomers within a tetramer and to avoid fluorescence fluctuations caused by in-plane rotations. The time trace clearly shows discrete and multiple intensity levels. Four different intensity levels (plus background) can be identified in the trace. The stepwise changes in fluorescence intensity as well as the intensity jumps between discrete levels are signatures of a multichromophoric system (20–23). As observed in Fig. 2*a*, the value of *P* also exhibited discrete (but minor) jumps that were correlated with intensity changes. This is more apparent in the correlation plot of Fig. 2*b*, in which the *P* values are plotted against the corresponding number of fluorescence counts (after background subtraction). *P* changed from 0.33 (±0.07) to 0.13 (±0.1) as the molecule jumped from the fourth to the third level. On the other three levels, *P* remained essentially constant. The maximum changes that *P* experiences corresponded to an effective in-plane angle of 6° (for this particular molecule). Fig. 2 *c* and *d* show the count histogram and the correlation plot (*P* vs. counts), of another

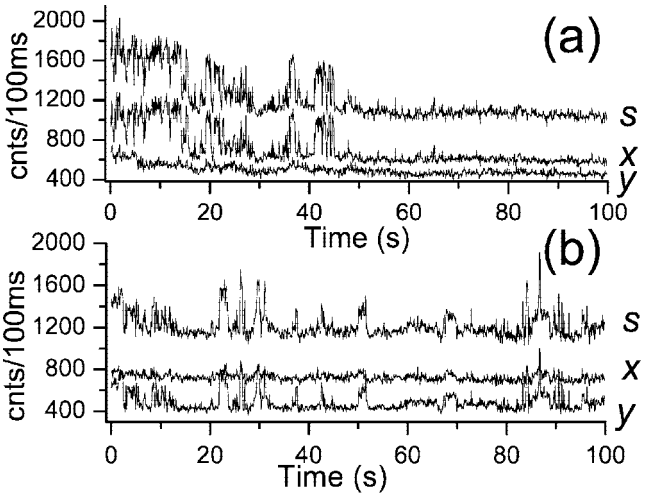

Fig. 3. Real-time fluorescence trajectories of two different DsRed proteins exhibiting blinking of a time scale of milliseconds to few seconds. Excitation intensity was 0.5 kW/cm^2 at 568 nm by using circularly polarized light. Acquisition time was 1 ms per point, with 100-ms binning time.

DsRed molecule. The histogram clearly indicates four different levels for this particular molecule. The correlation plot in Fig. 2*d* showed again a rather constant *P* emission with an average value of −0.4. In fact, for a total of 70 DsRed molecules investigated, we found no changes in the in-plane angle >6°.

In addition to multiple intensity levels, the fluorescence trajectories of the DsRed exhibited the characteristic "on–off" blinking of single-molecule experiments (24). Fig. 3 shows time traces of two different DsRed molecules with multiple intensity steps as well as "on–off" blinking on time scales comparable to those observed in the S65T mutant of the GFP (17). It is interesting to note the character of both polarization emission and blinking in the time traces. First, there were no changes in the polarization emission in time. The fluorescence emission of the tetramer was mainly along the *x*-direction in Fig. 3*a* but along the *y*-direction in Fig. 3*b*. Second, blinking occurred from a fluorescent level down to the background. Of the molecules investigated, 50% exhibited such blinking dynamics. To explain the occurrence of one-step blinking in DsRed, one would have to postulate that the four chromophores simultaneously jump to an "off" state, or that the chromophores are coupled in some fashion, as suggested by Lounis *et al.* (8), so that the resultant emission and on–off blinking proceed from one emitter in the complex. Intensity jumps to the background have also been observed in strongly coupled multichromophoric systems and are understood in terms of photogenerated traps, which quench the fluorescence of all of the other subunits (20–23).

Fluorescence Trajectories Analysis. The time trace shown in Fig. 2 is consistent with the notion of DsRed being a tetramer composed of four red subunits. Of 122 DsRed time trajectories analyzed, we found that 73% of the molecules displayed more than one intensity level, whereas 27% showed one-step behavior. The percentage of molecules displaying one to four levels is shown in Fig. 4*a Inset*. Surprisingly, only 14% of the molecules investigated exhibited four discrete levels. Further analysis of the fluorescence trajectories revealed that the changes in the fluorescence intensity were not of equal magnitude. The total fluorescence intensity distribution for the 122 DsRed molecules investigated is given in Fig. 4*a*. The ratio of the peak intensities follows a relation 4:2.6:1.5:0.7, instead of 4:3:2:1 as expected for equidistant intensity levels (the ratio is slightly different if one considers only the molecules showing four levels, namely: 4:2.5:1.5:0.5). The unequal reduction of intensity

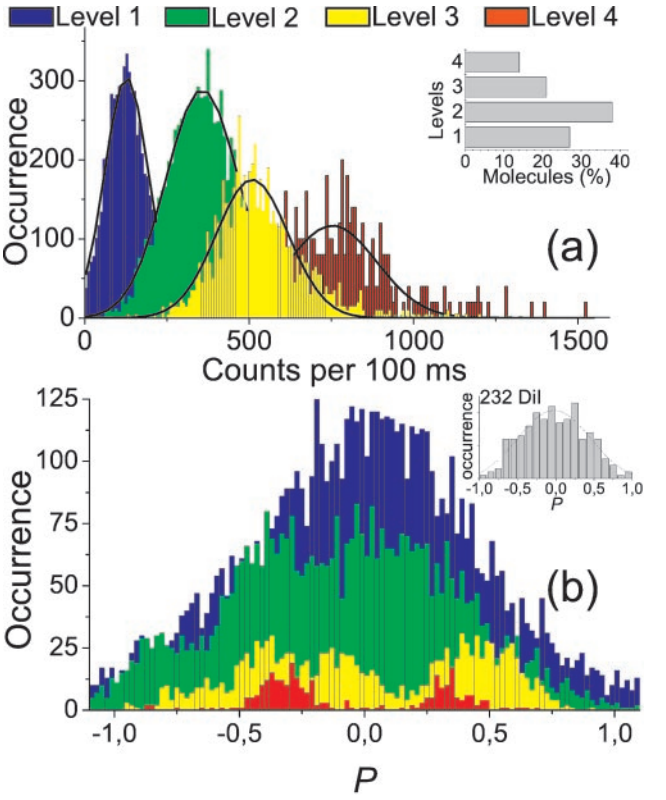

Fig. 4. (*a*) Fluorescence intensity distribution for 122 DsRed molecules excited with circularly polarized light at 568 nm. To compare the intensity levels between different trajectories, each recorded signal has been normalized to the excitation intensity with background subtraction. The histogram has been constructed after analyzing, one by one, all of the trajectories and building independent distributions for each intensity level. In the case of molecules showing only one or two levels, the assignment to a particular distribution was done by looking at its normalized intensity level after background subtraction and including it in the best-fitting distribution. The peak intensities of the four count distributions are: 966 (w = 338), 633 (w = 267), 357 (w = 220), and 163 (w = 170) for fourth, third, second, and first levels, respectively. *a Inset* shows the percentage of molecules displaying four, three, two, and only one intensity level. (*b*) *P* distribution of all four different levels for the same number of molecules as in *a*. For comparison, *b Inset* shows the *P* distribution for 232 1,1′-dioctadecyl-3,3,3′,3′-tetramethylindocarbocyanine molecules embedded in a thin polymer film. The width of the distribution reflects the random orientation of individual transition dipoles, as expected for single molecules embedded in an amorphous matrix. The *P* distributions for the first and second levels display similar width, whereas for the third and fourth levels, a dip develops around $P = 0$.

cannot be explained by solely orientational effects and suggests some fluorescence quenching within the complex. Weak quenching of the fluorescence has been observed in other multichromophoric systems and is attributed to coupling between closely interacting chromophores (20–23). Fig. 4*b* shows the distribution of the degree of polarization for the four different levels. The first and second levels exhibit a distribution characteristic of single emitter data, as can be seen from the comparison with the *P* distribution of individual carbocyanine molecules embedded in a thin polymer film (Fig. 4*b Inset*). Molecules with an out-of-plane emission component contribute equally to both detection channels when using a high N.A. objective, biasing *P* toward 0. See, for instance, ref. 25. Although statistics for the third and fourth levels are poor, because of both the low occurrence of molecules with these levels and their relatively short time duration, the distribution tends to develop into a symmetric double feature.

Ensemble Photobleaching Experiments. To verify the existence of photogenerated traps that would quench the fluorescence within

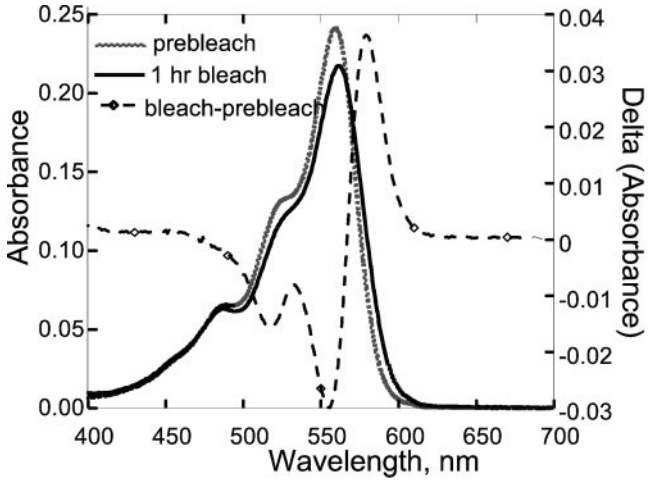

Fig. 5. Absorption spectra of DsRed taken before (gray dotted line) and after (black line) 1 h of continuous irradiation at 568 nm. The dashed line results from subtraction of both spectra showing photobleaching in the absorption peak at 568 nm and the generation of new species red-shifted with respect to the unbleached sample.

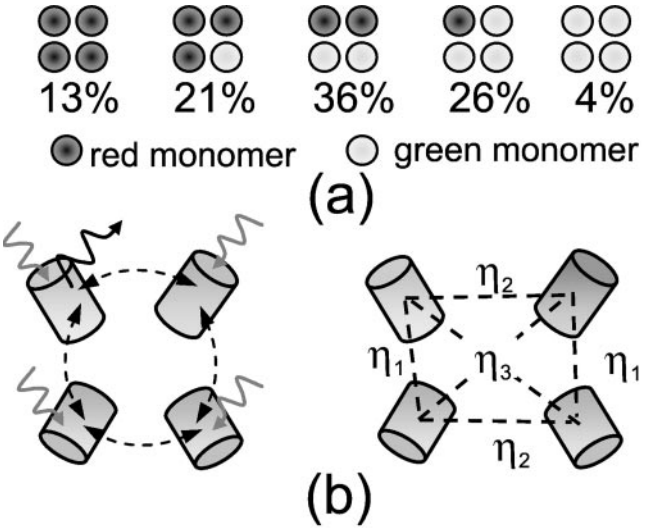

Fig. 6. (*a*) Distribution of red and green species within the DsRed, as derived from single-molecule data. (*b*) The cartoon illustrates the mechanism of fluorescence in DsRed. For simplicity, only red species are considered. (*Left*) Energy transfer occurs between all chromophores, and emission results with equal probability in time from any of the four chromophores. (*Right*) A damaged chromophore absorbs efficiently but partially quenches the fluorescence of the remaining undamaged chromophores. η_1, η_2, and η_3 are the quenching fractions for the nearest, intermediate, and most distant pairs, respectively.

the tetramer, we determined whether new absorption products would be generated during prolonged irradiation at 568 nm. The absorption spectrum after 1 h of continuous irradiation is shown in Fig. 5. As suspected, new red-shifted species were photogenerated, with an absorption peak resonant with the emission maximum of the prebleached DsRed. A minor fraction of blue-shifted species was also created at ≈530 nm, the middle shoulder in the DsRed absorption spectrum. Our results are consistent with recent bulk experiments by Cotlet *et al.* (26), in which newly absorbing and weakly fluorescent red shifted species were generated after prolonged irradiation at 543 nm.

Discussion

Stoichiometry of DsRed. Of the DsRed molecules investigated with two-color excitation, 83% emitted fluorescence above 590 nm with excitation both at 488 and 568 nm. On the basis of the observation from different groups (7, 10, 14), it seems improbable that at 488 nm we would be exciting the tail of the vibronic manifold of the red species. The verification of this hypothesis, however, requires thorough spectroscopic investigation of DsRed. Considering that direct excitation of red species at 488 nm is negligible, all of the fluorescence detected in the red on excitation at 488 nm would then arise from energy transfer between green and red species within the tetramer. From the dual color excitation experiments, we observed that 12.5% of the molecules emitted fluorescence only when excited at 568 nm, implying that they form the fraction of fully red species. This small percentage of red species is nicely consistent with our single-molecule trajectories at 568 nm excitation, where only 14% of the molecules exhibited four intensity levels. Considering the relative orientations of the dipole emission of DsRed taken from the crystallographic data (12), and projecting the vectors into the laboratory frame, we would still expect as many as 54% of the molecules to show four intensity levels if all monomers were red. The smaller value obtained (14%) is a direct indication of "missing" red species within most tetramers. We also observed 4% of the DsRed molecules showing emission only after excitation in the green. They should correspond to the fraction of fully green species, whose fluorescence tail in the red is detected. Combining all the data, we determine the stoichiometry for DsRed. Fig. 6*a* shows the results as taken directly from the percentages of molecules showing four, three, two, and one levels in the fluorescence trajectories and renormalizing to 100% to include the small percentage of only green species, as obtained from the images. To estimate the ratio r of red-to-green species, we calculated the probability of having four, three, two, one, and no red monomers in the tetramer for different values of r, assuming stochastic composition. The 13% of fully red tetramers corresponds to $r = 1.5$, whereas a fit to the total stoichiometry results in $r = 1.2$–1.5, which is very close to the values anticipated by Gross *et al.* (10) and Yarbrough *et al.* (12). For this ratio, the probabilities are: 11, 32, 36, 18, and 3.5% for four, three, two, one, and no red monomers, respectively, which agrees reasonably well with the experimental data.

It is important to recall that our model assumes that DsRed is a tetramer. The assumption is based on the crystallographic data (11, 12), the single-molecule experiments at concentrations as low as 10^{-9} and 10^{-10} M (8, 18), which also show multistep emission, and the oligomer dissociation constant of DsRed of $<10^{-9}$ M (6), which is one order of magnitude lower than the protein concentration used in our near-field scanning optical microscope experiments. We point out that premature photobleaching of species before recording the fluorescence emission is negligible. In average, we imaged a molecule for ≈125 ms, which is only a fraction (≈0.2%) of the total time we recorded its fluorescence emission.

Recently, Cotlet *et al.* (18) reported that 40% of their DsRed molecules exhibited four levels. Except for the use of a different matrix to immobilize the proteins, their experimental conditions are similar to ours. In contrast, Lounis *et al.* (8) reported only 10% of molecules showing three or four steps in the intensity, although no experimental details concerning the polarization of the excitation light were given. However, the excitation intensity levels were more than one order of magnitude higher than in our experiments, which might have resulted in the photobleaching of many of the monomers before actual recording of the fluorescence.

Mechanism for the Red Fluorescence in DsRed. The multiple-step behavior of the fluorescence emission with constant P values, the weak quenching of the fluorescence emission on photodissociation of one of the chromophores, and the one-step off-blinking are all consistent with a model that includes coupling between the different chromophores of the tetramer. Fig. 6*b* illustrates

with a cartoon the possible mechanism that governs the emission of fluorescence in DsRed. Under the low-excitation conditions used in our experiments, we do not consider simultaneous excitation of two or more chromophores within one complex. According to our model, all red species within a tetramer will absorb light with the same probability. Energy transfer between the identical chromophores will occur via coupling of the transition dipoles of the individual subunits and with the emission proceeding from one of the chromophores of the complex. Considering that the rates of energy transfer between subunits, calculated on the basis of the crystallographic data, are much faster that the fluorescence rate (8), the emission is essentially equally likely to arise from any of the four chromophoric units. Within the time scale of our experiments (1-ms integration time), the energy will be redistributed among all subunits, resulting in an "average" value for polarization emission. The small jumps in P on intensity changes are indicative of a redistribution of energy among the monomers, which is visualized as a partial depolarization of the whole complex. A similar model has been also hypothesized by Lounis *et al.* (8). For the highest levels (third and fourth), the P distributions show bimodal shape, which is consistent with the distribution one finds when simulating a four-emitter system with fixed angles between their respective dipoles. Furthermore, on photodissociation of one of the chromophores, the remaining fluorescence is substantially reduced, and bulk experiments show that on prolonged irradiation in the red band, weakly fluorescent species with an absorbing band resonant with the emission maxima of the prebleached DsRed are generated. Both results are consistent with the notion that on photodissociation, the chromophore converts into a different species, which still absorbs efficiently, acting like a trap for the energy of the absorbed photon partially quenching the fluorescence of the remaining subunits. From the single-molecule data, we find that the peak intensities follow a ratio of $\approx$4:2.6:1.5:0.7. Assuming that chromophore i quenches a η_i fraction of the fluorescence on its dissociation (see Fig. 4*b*), we calculate η_i among different pairs, taking into account the distance and relative orientations between different monomers, as extracted from the crystallographic data (11, 12). The best fit to our fluorescence levels occurs with $\eta_1 = 0.27$, $\eta_2 = 0.06$, and $\eta_3 = 0.002$ for the nearest, intermediate, and most distant pairs, respectively, with a total quenching efficiency of $\Sigma\eta_i = 0.33$. The one-step off-blinking observed in DsRed is understood by using similar arguments. Energy transfer from any of the absorbing chromophores to a "dark state" within the tetramer complex will occur much faster and more efficiently than emission of the fluorescence, resulting in total but reversible quenching of the fluorescence. The origin of the dark states or reversible photon traps responsible for on–off blinking in autofluorescent proteins is not yet understood (16, 17, 24).

Interestingly, we note that a tetrameric ordered ensemble of strongly absorbing chromophores, like the DsRed tetramer, suggests that the molecular exciton model (27, 28) of excitation transfer might be active. A first estimate for the pair separated by 22 Å yields 18-cm^{-1} interaction energy (M. Kasha, personal communication), which is above the estimated upper limit for Förster interaction energy given by Förster (29) in his comparison of the two models. An exploratory study of this possibility could lead to unraveling the molecular basis of the "maturing effect" of the red tetramer.

Conclusion

We have used single-molecule detection to study the fluorescence emission in DsRed. Real-time fluorescence trajectories with 1-ms time resolution have been obtained by using a polarization-sensitive near-field scanning optical microscope. In addition, dual color excitation experiments at 488 and 568 nm and detection in the red have been conducted to assess the ratio of red-to-green species in DsRed. From combined real-time trajectories and dual-color microscopy data, we deduce a red-to-green monomer ratio of 1.2–1.5, assuming a tetramer structure. Furthermore, the single-molecule data are consistent with a model in which energy transfer between chromophores occurs efficiently and with the emission proceeding with equal probability from any of the four chromophores. We also observed weak quenching of the fluorescence on photodissociation of a chromophore in the complex. On the basis of these results, we anticipate that oligomer suppression in DsRed not only will make the protein more suitable for biological applications but also will enhance its fluorescence brightness. Moreover, in view of the red-to-green ratio obtained, the extinction coefficient of fully red DsRed tetramers at 568 nm should be about two times larger than reported by Baird *et al.* (7).

We are indebted to M. Kasha for valuable and joyful discussions. We thank J. Hofkens and M. Cotlet for communication of data before publication and T. Jovin for careful reading of the manuscript. We thank B. I. de Bakker, J. Korterik, F. B. Segerink, W. H. J. Rensen, and L. Kuipers for assistance and helpful suggestions. The research of M.F.G.-P. was made possible by a fellowship of the Royal Netherlands Academy of Arts and Sciences. M.K. and E.M.H.P.vD. are supported by the Netherlands Foundation for Fundamental Research of Matter.

1. Matz, M. V., Fradkov, A. F., Labas, Y. A., Savitsky, A. P., Zaraisky, A. G., Markelov, M. L. & Lukyanov, S. A. (1999) *Nat. Biotechnol.* **17**, 969–973.
2. Chalfie, M. Y., Euskirchen, Tu. G., Ward, W. W. & Prasher, D. C. (1994) *Science* **263,** 802–805.
3. Tsien, R. Y. (1998) *Annu. Rev. Biochem.* **67,** 509–544.
4. Fradkov, A. F., Chen, Y., Ding, L., Barsova, E. V., Matz, M. V. & Lukyanov, S. A. (2000) *FEBS Lett.* **479,** 127–130.
5. Mizuno, H., Sawano, A., Eli, P., Hama, H. & Miyawaki, A. (2001) *Biochemistry* **40,** 2502–2510.
6. Heikal, A. A., Hess, S. T., Baird, G. S., Tsien, R. Y. & Webb, W. W. (2000) *Proc. Natl. Acad. Sci. USA* **97,** 11996–12001.
7. Baird, G. S., Zacharias, D. A. & Tsien, R. Y. (2000) *Proc. Natl. Acad. Sci. USA* **97,** 11984–11989.
8. Lounis, B., Deich, J., Rosell, F. I., Boxer, S. G. & Moerner, W. E. (2001) *J. Phys. Chem. B* **105,** 5048–5054.
9. Jakobs, S., Subramaniam, V., Schonle, A., Jovin, T. M. & Hell, S. W. (2000) *FEBS Lett.* **479,** 131–135.
10. Gross, L. A., Baird, G. S., Hoffman, R. C., Baldridge, K. K. & Tsien, R. Y. (2000) *Proc. Natl. Acad. Sci. USA* **97,** 11990–11991.
11. Wall, M. A., Socolich, M. & Ranganathan, R. (2000) *Nat. Struct. Biol.* **7,** 1133–1138.
12. Yarbrough, D., Wachter, R. M., Kallio, K., Matz, M. V. & Remington, S. J. (2001) *Proc. Natl. Acad. Sci. USA* **98,** 462–467.
13. Volkmer A., Subramanim V., Birch, D. J. & Jovin, T. M. (2000) *Biophys. J.* **78,** 1589–1598.
14. Schöttrigkeit, T. A., Zachariae, U., von Feilitzsch, T., Wiehler, J., von Hummel, J., Steipe, B. & Michel-Beyerle, M. E. (2001) *ChemPhysChem* **2,** 325–328.
15. Weiss, S. (1999) *Science* **283,** 1676–1683.
16. Dickson, R. M., Cubitt, A. B., Tsien, R. Y. & Moerner, W. E. (1997) *Nature (London)* **388,** 355–358.
17. Garcia-Parajo, M. F., Segers-Nolten, G. M. J., Veerman, J. A. Greve, J. & van Hulst, N. F. (2000) *Proc. Natl. Acad. Sci. USA* **97,** 7237–7242.
18. Cotlet, M., Hofkens, J., Köhn, F., Michiels, J., Dirix, G., van Guyse, M., Vandetleyden, J. & De Schryver, F. C. (2001) *Chem. Phys. Lett.* **336,** 415–423.
19. Van Hulst, N. F., Veerman, J. A., Garcia-Parajo, M. F. & Kuipers, L. (2000) *J. Chem. Phys.* **112,** 7799–7809.
20. Vanden Bout, D. A., Yip, W.-T., Hu, D., Fu, D.-K., Swager, T. M. & Barbara, P. F. (1997) *Science* **277,** 1074–1077.
21. Bopp, M. A., Jia, Y., Li, L., Cogdell, R. J. & Hochstrasser, R. M. (1997) *Proc. Natl. Acad. Sci. USA* **94,** 10630–10635.
22. Ying, L. & Xie, X. S. (1998) *J. Phys. Chem.B.* **102,** 10399–10409.
23. Hofkens, J., Maus, M., Gensch, T., Vosch, T., Cotlet, M., Köhn, F., Herrmann, A., Müllen, K. & De Schryver, F. C. (2000) *J. Am. Chem. Soc.* **122,** 9278–9288.
24. Moerner, W. E. (1997) *Science* **277,** 1059.
25. Ha, T., Laurence, T. A., Chemla, D. S. & Weiss, S. (1999) *J. Phys. Chem. B* **103,** 6839–6850.
26. Cotlet, M., Hofkens, J., Habuchi, S., Dirix, G., van Guyse, M., Michiels, J., Vanderleyden, J. & De Schryver, F. C., (2001) *Proc. Natl. Acad. Sci. USA* **98,** 14398–14403. (First Published November 27, 2001; 10.1073/pnas.251532698)
27. Davydov, A. S. (1962) *Theory of Molecular Excitons* (McGraw–Hill, New York).
28. Kasha, M. (1975) in *Spectroscopy of the Excited State*, ed. Di Bartolo, B. (Plenum, New York), pp. 337–363.
29. Förster, Th. (1960) in *Comparative Effects of Radiation*, eds. Burton, M., Kirby-Smith, J. S. & Magee, J. C. (Wiley, New York).